RESEARCH ARTICLE

ScienceAsia 30 (2004): 191-203

A Multi-segment Mathematical Model with Variable Compliance for Pressure Controlled Ventilation

Konvika Kongkul,[a,c] Sahattaya Rattanamongkonkul[a,c,d,*] and Philip S Crooke[b]

[a] Department of Mathematics, Mahidol University, Bangkok 10400, Thailand.
[b] Department of Mathematics, Vanderbilt University, Nashville, TN 37240, USA.
[c] Supported by a scholarship under the Ministry Staff Development Project of Ministry of University Affairs, Thailand.
[d] Supported by the Thailand Research Fund and the National Research Council of Thailand.

[*] Corresponding author, E-mail: g4336633@student.mahidol.ac.th

Received 15 Nov 2003
Accepted 8 Mar 2004

ABSTRACT: A mathematical model with multi-segment variable compliance which describes the volume of a single compartment lung for pressure controlled ventilation has been proposed and compared against a constant compliance model. The compliance in the constant compliance model is the average of those in the variable compliance model. In our model, on the other hand, a variable compliance is approximated by piecewise linear function of the lung volume. The model was then used to compute the outcome variables of clinical interest; tidal volume, average volume, end-expiratory pressure, and mean alveolar pressure. Using data obtained from healthy and injured pigs, the variable compliance model was used to study effects of recruitment maneuvers on the key outcome variables. Furthermore, the limiting value for each outcome variable was derived as a function of the physiologic and ventilatory parameters.

KEYWORDS: pressure controlled ventilation; mathematical model; multi-segment; variable compliance.

INTRODUCTION

Respiratory failure has become an important health problem, especially in a disease called acute respiratory distress syndrome (ARDS) which can harm and destroy the respiratory system. Many patients who suffer from this disorder need mechanical ventilation to aid breathing whenever they are not able to move enough air in and out of their lungs. Many types of ventilators and modes of operation may be used for the treatment. Pressure controlled ventilation is most often prescribed for patients with severe ARDS.[1,2]

The mechanism of respiration has gained increasing importance in the study of guidelines for ventilator settings in order to protect the lungs from damage. Many mathematical models for mechanical ventilation have been developed.[3-10] The models are generally broken down into single compartment models and multi-compartment models. These models allow the resistances for inspiration and expiration to be different, incorporating positive end-expiratory pressure (PEEP), and covering the basic clinical modes of ventilation. However, most of these models have assumed the same constant compliance for the inspiratory and expiratory phases. The dynamics of the elastic pressure-volume (P_{el}-V) curves have also been studied extensively.[11-16] Based on a study of Svantesson *et al.* in 1998,[13] a three-segment variable compliance model for pressure controlled ventilation was proposed by Crooke *et al.* in 2002.[17]

Oleic acid-injured animal models are used widely to test a variety of adjunctive therapies in mechanical ventilation.[18-20] Using animal models as a proxy for lung injury and disease, researchers have probed the effects of various therapeutic techniques, ranging from liquid ventilation,[21] splanchnic perfusion and oxygenation,[22] ventilatory support[23-25] to tracheal gas insufflation (TGI).[26] One of the more prominent usages of oleic acid-injury models is in studies of recruitment.[23,27,28] The mathematical model developed in this paper is based on a subset of data collected from twenty pigs that were subjected to mechanical ventilation before and after oleic acid injury. The experimental protocol for the animal studies was approved by the Animal Care

and Use Committee of Regions Hospital. In order to study mechanical ventilation, the experiments were carried out by using monitoring equipments. The (P_{el}-V) data was collected without applied positive end-expiratory pressure (PEEP = 0) during inspiration and expiration from pre- and post-injury pigs. The collected (P_{el}-V) data for each pre- and post-injury pig showed that the injury has an effect on the lung compliance. Therefore, we constructed a multi-segment mathematical model for pressure controlled ventilation with variable compliance, based on a single compartment model. Using the experimental (P_{el}-V) data from pre- and post-injury pigs, the lung's variable compliance could be approximated by a piecewise linear function of the lung volume, V. Next, this model was compared to a linear model with constant compliance of pressure controlled ventilation which served to link the clinical input variables, namely pressure level, frequency, inspiratory time fraction, and impedance, with key outcome variables of clinical interest, such as tidal volume, average volume, end-expiratory pressure, and mean alveolar pressure.

Furthermore, for traditional modes of ventilation, the tidal volume (V_T), minute ventilation (V_E), end-expiratory pressure (P_{ex}), mean alveolar pressure (P_m), and power (W_m) are asymptotic to finite limiting values as the cycling frequency f becomes sufficiently large.[5,29,30] It is therefore informative to calculate these limiting values as $f \to \infty$, in order to make some clinically relevant observations concerning these important key outcome variables. Such linkages between these key outcome variables (V_T,V_E, P_{ex}, P_m and W_m) and the physiologic variables (compliances and resistances) as $f \to \infty$ will provide limits or bounds for these quantities, which can assist clinicians in the optimization of the desired outcomes on a particular clinical settings.

Previous Model

The mathematical model for pressure controlled ventilation incorporates pressure support ventilation that is applied to a single lung with compliance C, inspiratory resistance R_i, and expiratory resistance R_e. The ventilator cycle is split into two parts: inspiration of duration t_{in} and expiration of duration t_{ex}. The total length of each cycle is $t_{tot} = t_{in} + t_{ex}$.

One compartment models for mechanical ventilation are formed by assuming a pressure balance within the compartment:

$$P_r + P_{el} + P_{res} = Pvent \qquad (1)$$

in which the pressure balance at any time t during each period of breathing cycle is composed of pressures due to resistive losses (P_r), pressures due to elastic forces (P_{el}), residual pressures (P_{res}), and applied pressures to the compartment (P_{vent}). During inspiration, a pressure P_{set} is applied to the airway, $P_{vent} = P_{set}$, and during expiration, the ventilator applies a constant pressure P_{peep},P_{vent}=P_{peep}.

In actual fact, the lungs cannot be emptied of gas, even by the most forceful expiration. Some gas still remains as the residual volume. We define the end-expiratory volume (V_{ex}) to be the volume of the lung above its residual volume during a maximal forced expiration that starts at the end of a normal tidal expiration. $V(t)$ denotes the volume of the compartment above V_{ex} at any time t. During each breathing cycle, $V_i(t)$ and $V_e(t)$ denote the volumes of the compartment above its residual volume during inspiration and expiration, respectively. We then assume that

$$P_{el} = \frac{V}{C(V + V_{ex})}$$

where $C(V+V_{ex})$ is the compliance function for the elastic pressure. The residual pressure called the end-expiratory pressure, P_{ex}, is the pressure due to V_{ex}. The relationship between V_{ex} and P_{ex} is given by

$$P_{ex} = \frac{V_{ex}}{C(V_{ex})}.$$

For the resistive pressure, we assume that

$$P_r = RQ^{\varepsilon},$$

where Q is the flow into or out of the lung, that is,

$$Q = \left|\frac{dV}{dt}\right|,$$

R is a constant, and ε is a positive parameter. With these assumptions, the volume of the compartment is given by the following differential equations.

Inspiration

$$R_i\left(\frac{dV_i}{dt}\right)^{\varepsilon_i} + \frac{V_i}{C_i(V_i + V_{ex})} + P_{ex} = P_{set},\ 0 \le t \le t_{in} \qquad (2)$$

Expiration

$$-R_e\left(\left|\frac{dV_e}{dt}\right|\right)^{\varepsilon_e} + \frac{V_e}{C_e(V_e + V_{ex})} + P_{ex} = P_{peep},\ t_{in} < t \le t_{tot}. \qquad (3)$$

In equations (2) and (3), the unknown resistances R_i and R_e can be obtained from the experimental data by plotting resistive pressure against flow and fitted with a least-squares curve.[6] The initial conditions for the model equations (2) and (3) are $V_i(0) = 0$ and $V_e(t_{in}) = V_T$, respectively, where V_T is the tidal volume. The constant P_{ex} is determined by the equation $V_e(t_{tot}) = 0$.

The solutions of the simplest model for pressure controlled ventilation when $\varepsilon_i = \varepsilon_e = 1$ and

$$C_i(V_i + V_{ex}) = C_e(V_e + V_{ex}) \equiv C,$$

where C is a constant compliance, and can be derived easily.[5,29] Other solutions of model equations (2) and

(3), with constant compliance and $\varepsilon_i = \varepsilon_e = \frac{1}{2}$ or 2, were found by Crooke and Marini in 1993.[6] Most other researchers put $\varepsilon_i = \varepsilon_e = 1$ finding that their models work reasonably well and are more mathematically tractable.[3,5,6-10,17] In 2002, Crooke *et al.*[17] proposed, solved and analyzed a one-segment mathematical model for pressure controlled ventilation with variable compliance. Their one-segment model is of the form given in equations (2) and (3), when $\varepsilon_i = \varepsilon_e = 1$,

$$C_i(V_i + V_{ex}) = a_i + b_i(V_i + V_{ex}),$$

and

$$C_e(V_e + V_{ex}) = a_e + b_e(V_e + V_{ex}),$$

where a_i, b_i, a_e and b_e are parameters obtained from P_{el}-V the curves. That is,

Inspiration

$$R_i\left(\frac{dV_i}{dt}\right) + \frac{V_i}{a_i + b_i(V_i + V_{ex})} + P_{ex} = P_{set},\ 0 \le t \le t_{in} \qquad (4)$$

Expiration

$$R_e\left(\frac{dV_e}{dt}\right) + \frac{V_e}{a_e + b_e(V_e + V_{ex})} + P_{ex} = P_{peep},\ t_{in} < t \le t_{tot}. \qquad (5)$$

Multi-Segment Model

In 2002, Crooke *et al.*[17] suggested a nonlinear mathematical model for pressure controlled ventilation called the three-segment model, in which the compliance of the compartment was allowed to be a piecewise linear function that varies with the compartment volume. Their compliance for each phase of breathing cycle was segmented into three parts, each of which varied linearly with volume up to a particular lung volume. In this paper, we attempt to improve the accuracy by proposing a multi-segment model in which the compliance for each part of the breathing cycle consists of multiple segments.

First, we consider the elastic pressure in the lung in its simplest form, that is

$$P_{el} = \frac{V}{C(V)} \qquad (6)$$

where P_{el} is the elastic pressure of a single compartment lung and V is the lung volume above its residual volume. The experimental P_{el}-V data for inspiration and expiration, pre- and post-injury pigs applied in this paper was collected without applied PEEP and the end-expiratory pressure, P_{ex}, of the lung was assumed to be zero. Then, the function $C(V)$, the compliance function of the model, is allowed to be a piecewise linear function over the inspiratory and expiratory phases for each breath. In particular, the compliance functions for inspiration $C_i(V)$ and expiration $C_i(V)$ of the multi-segment model, with J segments during inspiration and K segments during expiration, have the forms:

$$C_i(V) = \begin{cases} a_{i1} + b_{i1}V & \text{if} \quad 0 \le V \le v_{i1} \\ a_{i2} + b_{i2}V & \text{if} \quad v_{i1} \le V \le v_{i2} \\ \vdots & \\ a_{ij} + b_{ij}V & \text{if} \quad v_{i(j-1)} \le V \le V_T \end{cases} \qquad (7)$$

and

$$C_e(V) = \begin{cases} a_{ek} + b_{ek}V & \text{if} \quad 0 \le V \le v_{e(k-1)} \\ a_{e(k-1)} + b_{e(k-1)}V & \text{if} \quad v_{e(k-1)} \le V \le v_{e(k-2)} \\ \vdots & \\ a_{e1} + b_{e1}V & \text{if} \quad v_{e1} \le V \le V_T, \end{cases} \qquad (8)$$

where v_{ij} and v_{ek} denote the volumes at which the compliance function changes its form during inspiration and expiration, respectively. The constants v_{ij} and v_{ek}, where $j=1,2,..,J$ and $k=1,2,..,K$, as well as the numbers J and K are determined as those which yield the least-squares fitting of the collected P_{el}-V data.

Thus, the multi-segment approximation of the compliance functions as in equations (7) and (8) is used in order to obtain a more accurate fit. To test the accuracy of our model, a Mathematica program was written to accept the experimental P_{el}-V data and obtained a least-squares fit of the experimental data up to 5 segments in each part of the breathing cycle. The resulting curves are shown in Fig 1 for both pre- and post-injury cases of a particular pig. The parameters used in a five-segment fit of P_{el}-V curves in Fig 1 are listed in Table 1. In this table, the parameters, a_i, b_i, a_e, b_e, v_i and v_e for inspiration and expiration of pre- or post-injury pig for each segment are listed.

The basic one-segment model given in equations (4) and (5) has been generalized to a multi-segment model by assuming that the compliance functions $C_i(V)$ and $C_e(V)$ vary according to equations (7) and (8), which results in the following multi-segment model.

Inspiration

$$R_i\left(\frac{dV_{i_j}}{dt}\right) + \frac{V_{i_j}}{a_{ij} + b_{ij}(V_{i_j} + V_{ex})} + P_{ex} = P_{set},$$
$$t_{i_{(j-1)}} \le t \le t_{i_j},\ j = 1, 2, \ldots, J, \qquad (9)$$

Expiration

$$R_e\left(\frac{dV_{e_k}}{dt}\right) + \frac{V_{e_k}}{a_{ek} + b_{ek}(V_{e_k} + V_{ex})} + P_{ex} = P_{peep},$$
$$t_{in} + t_{e_{(k-1)}} < t \le t_{in} + t_{e_k}, \qquad (10)$$

where $t_{i0}=0=t_{e0}$, $t_{ij}=t_{in}$, and $t_{eK}=t_{ex}$. The initial and boundary

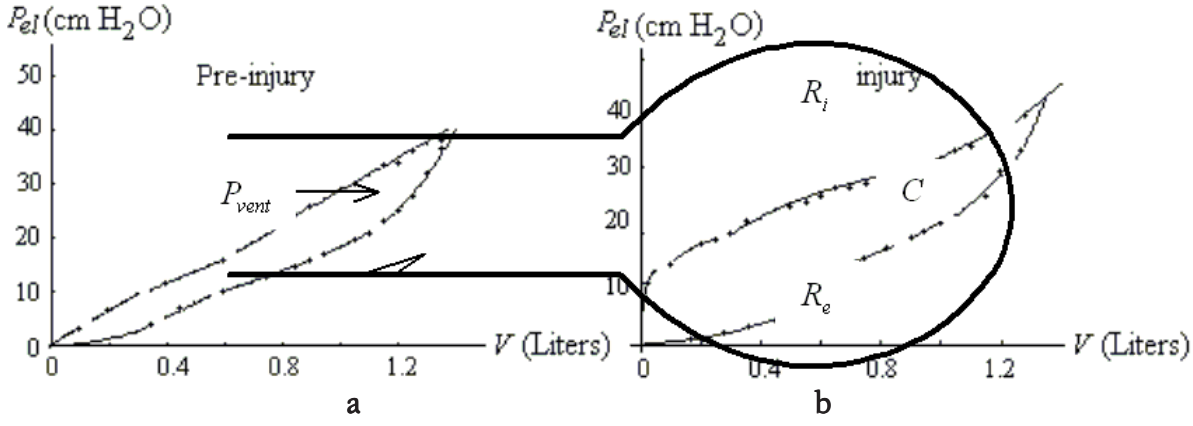

Fig 1. An example of P_{el}-V data for pre-injury (a) and post-injury (b) pig approximated by five-segment compliance functions. The dots represent P_{el}-V data obtained from the experiments, while the solid lines are the approximate P_{el}-V curves.

Table 1. The parameters *a, b* and *v* obtained from the least squares fit of experimental data using five-segment compliance functions during inspiration and expiration periods, for pre- and post-injury pig. The units for *a*, *b*, and *v* are L/cm H_2O, L/cm H_2O, and liter (L), respectively.

Segment	Parameters	Pre-injury		Post-injury	
		Inspiration	Expiration	Inspiration	Expiration
1	*a*	0.027363	0.237805	0.000641	0.143059
	b	0.012846	-0.435540	0.070513	-0.080896
	v	0.30	1.15	0.35	1.25
2	*a*	0.027451	0.182155	0.003172	0.097537
	b	0.016631	-0.268782	0.045721	-0.044771
	v	0.55	0.95	0.45	1.05
3	*a*	0.039757	0.065133	0.009588	0.070584
	b	-0.005182	-0.010138	0.024759	-0.019948
	v	0.80	0.60	0.95	0.90
4	*a*	0.042238	0.083840	0.026285	0.058010
	b	-0.008795	-0.029532	0.006863	-0.005957
	v	0.90	0.40	1.20	0.60
5	*a*	0.037296	0.147569	0.046200	0.248390
	b	-0.002475	-0.082240	-0.009205	-0.323795

conditions for the model equations (9) and (10) are $V_{i1} = 0$, $V_{ij}(t_{in}) = V_T$ and $V_{eK}(t_{tot}) = 0$, while the solutions are required to satisfy the continuity conditions

$$V_{i_j}(t_{i_j}) = V_{i_{(j+1)}}(t_{i_j}),\ j = 1, 2, \ldots, J-1,$$

and

$$V_{e_k}(t_{e_k}) = V_{e_{(k+1)}}(t_{e_k}),\ k = 1, 2, \ldots, K-1.$$

Applying the above continuity conditions, the following restrictions are to be placed on the parameters of compliance functions:

$$a_{i(j+1)} = a_{ij} + (b_{ij} - b_{i(j+1)})v_{ij} \qquad (11)$$

and

$$a_{e(k+1)} = a_{ek} + (b_{ek} - b_{e(k+1)})v_{ek}. \qquad (12)$$

The unknown P_{ex} is determined by the equation $V_{eK}(t_{tot}) = 0$. The parameters $v_{i1}, v_{i2}, \ldots, v_{i(J-1)}$, for inspiration, and , for expiration, are inputs of the model, and are obtained from the experimental data. The transition times, t_{ij} and t_{ek}, which appear in the model equations (9) and (10) are found from the equations $V_{ij}(t_{ij}) = v_{ij} - V_{ex}$ and $V_{e_k}(t_{e_k}) = v_{ek} - V_{ex}$, where $j = 1, 2, \ldots, J$ and $k = 1, 2, \ldots, K$, respectively, whenever these equations can be solved analytically for the transition times.[17]

In order to carry out the simulation of the multi-segment model, the numbers $J \leq 5$ and $K \leq 5$, of the segments for the variable compliance, which depend on the values of V_{ex} and V_T, are required. Depending on the values of V_{ex} and V_T, we then classify the segments during the inspiratory and expiratory periods by means of the values of the times t_{ij} and t_{ek}, and the compartmental volumes v_{ij} and v_{ek} as follows.

The five segments used in the simulation during the inspiratory period are

$$\left.\begin{array}{rll}
\text{1st segment:} & 0 \le t \le t_{i_1} & \text{and} \quad 0 \le V_i(t) \le v_{i1}, \\
\text{2nd segment:} & t_{i_1} \le t \le t_{i_2} & \text{and} \quad v_{i1} \le V_i(t) \le v_{i2}, \\
\text{3rd segment:} & t_{i_2} \le t \le t_{i_3} & \text{and} \quad v_{i2} \le V_i(t) \le v_{i3}, \\
\text{4th segment:} & t_{i_3} \le t \le t_{i_4} & \text{and} \quad v_{i3} \le V_i(t) \le v_{i4}, \\
\text{and, 5th segment:} & t_{i_4} \le t \le t_{in} & \text{and} \quad v_{i4} \le V_i(t) \le V_T.
\end{array}\right\} \qquad (13)$$

Similarly, the five segments used in the simulation during the expiratory period are

$$\left.\begin{array}{rll}
\text{1st segment:} & t_{in} \le t \le t_{in} + t_{e_1} & \text{and} \quad 0 \le V_e(t) \le v_{e4}, \\
\text{2nd segment:} & t_{in} + t_{e_1} \le t \le t_{in} + t_{e_2} & \text{and} \quad v_{e4} \le V_e(t) \le v_{e3}, \\
\text{3rd segment:} & t_{in} + t_{e_2} \le t \le t_{in} + t_{e_3} & \text{and} \quad v_{e3} \le V_e(t) \le v_{e2}, \\
\text{4th segment:} & t_{in} + t_{e_3} \le t \le t_{in} + t_{e_4} & \text{and} \quad v_{e2} \le V_e(t) \le v_{e1}, \\
\text{and, 5th segment:} & t_{in} + t_{e_4} \le t \le t_{tot} & \text{and} \quad v_{e1} \le V_e(t) \le V_T.
\end{array}\right\} \qquad (14)$$

Hence, 225 cases are possible depending on whether v_{ij} or v_{ek} exceed , V_T or V_{ex}, when attempting to obtain the best fit. A Mathematica program was written for the multi-segment model that covers these 225 cases to calculate the lung volume over one breathing cycle for parameter settings obtained above. From the above conditions shown in the expressions (13) and (14), five segments will be applied to both inspiration and expiration in the model simulation if $0 < V_{ex} < v_{i1}$, $v_{i4} < V_T$, $0 < V_{ex} < v_{e4}$ and $v_{e1} < V_T$.

In Fig 2, the resulting $P_{el} - V$ curves subjected to the continuity conditions (11) and (12) are shown for both pre- and post-injury cases of a particular pig. The parameters used in this data fitting are as listed in Table 1. The compliance functions in the simulations of the $P_{el} - V$ curves shown in Fig 2 are presented in Fig 3. In Figs 2 and 3, the dashed lines indicate the volumes at which the compliance function changes its form, while the solid vertical lines in the graphs shown in Figure 3 indicate the values of V_{ex} and $V_T + V_{ex}$.

A simulation of the multi-segment variable compliance model can be seen as solid curves in Figure 4, which shows the lung volume over one breathing cycle for pre- and post-injury cases using the parameter values given in Table 1 obtained by curve fitting of the $P_{el} - V$ data shown in Fig 1. In this simulation, the compliance functions for inspiration and expiration are different. Here, in the pre-injury case, four segments are used for inspiration period and two segments are used for expiration period since we have and during inspiration, while and during expiration. In the post-injury case, on the other hand, two segments are used for inspiration period and one segment is used for expiration period since we have $v_{i1} < V_{ex} < v_{i2}$ and $v_{i4} < V_T$ during inspiration, while $v_{e4} < V_{ex} < v_{e3}$ and $v_{e3} < V_T < v_{e2}$ during expiration in the post-injury case. Then, the segments numbered 2-5 and numbered 1-2 as shown in equation (13) are used in the simulation during inspiration for pre- and post-injury cases, respectively, while the segments numbered 2-3 and numbered 1 as shown in equation (14) are used in the simulation during expiration for pre- and post-injury cases, respectively. Therefore, for both pre- and post-injury cases, the multi-segment models are of the form given in equations (9) and (10), where j = 2,3,4,5 and k = 2, 3, for pre-injury case, while for post-injury case, j = 1,2 and k = 1. Here, we assume t_{i1} = 0 and t_{i0} = 0 as the starting times for the inspiration period in the pre- and post-injury cases, respectively, and t_{e1} = 0 and t_{e0} = 0 as the starting times for the expiration period in both pre- and post-injury cases. Also, $t_{i5} = t_{in}$, $t_{i2} = t_{in}$, $t_{e3} = t_{ex}$ and $t_{e1} = t_{ex}$ as the ending times for the inspiration and expiration periods for both pre- and post-injury cases.

Having the compartment volume, the key outcome variables of the clinical interest; namely, tidal volume

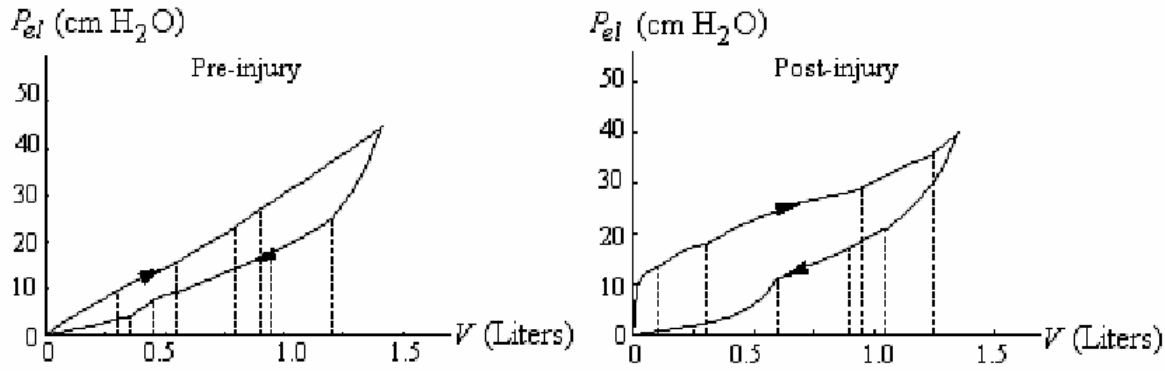

Fig 2. Continuous P_{el}-V curve for pre-injury (a) and post-injury (b) pig using five-segment approximating compliance function subject to continuity conditions (11) and (12). The arrow indicates inspiration (↗) or expiration (↙).

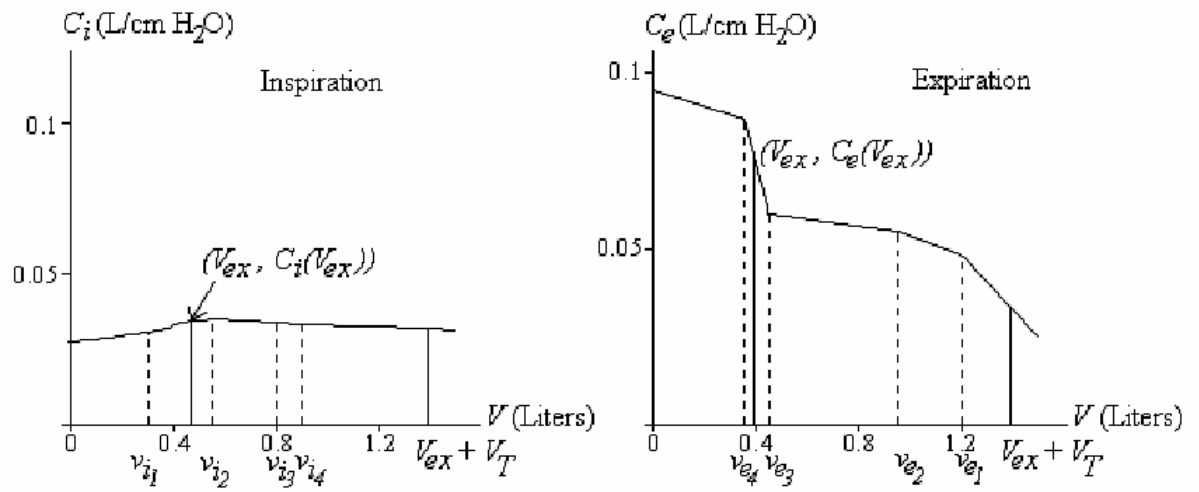

Fig 3. Compliance functions used in Fig 3. The dashed lines indicate the volumes at which the compliance function changes its form and the solid lines indicate V_{ex} and V_T+V_{ex}.

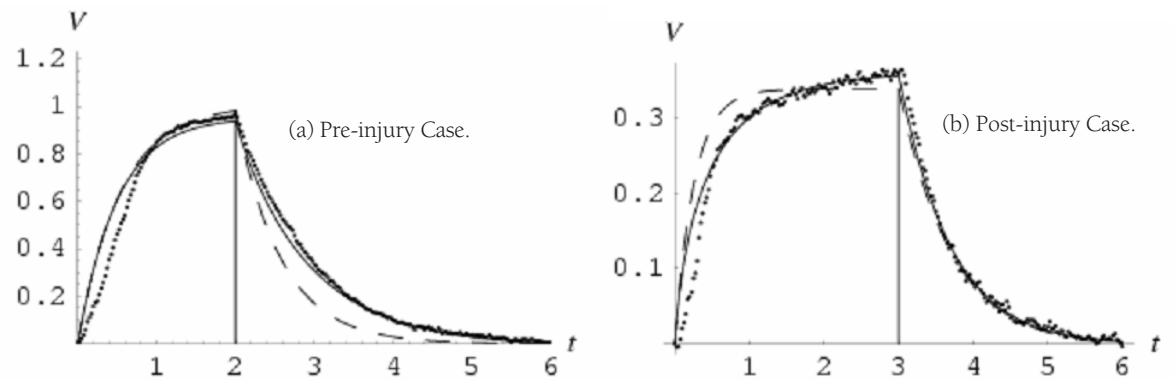

Fig 4. Comparison of constant compliance and multi-segment variable compliance models. Here, the lung volume curves are simulated over one breath by multi-segment model, in pre-injury case (a) with P_{set}=35 cm H_2O, P_{peep}=5, t_{tot}=6s, t_{in}=2s, R_i=16 cm H_2O/L/s and R_e=17 cm H_2O/L/s, and in post-injury case (b) with P_{set}=35 cm H_2O, P_{peep}=15, t_{tot}=6s, t_{in}=3s, R_i=13.75 cm H_2O/L/s and R_e=14.25 cm H_2O/L/s. The solid curves correspond to the lung volume obtained from the multi-segment models, and the dashed curves correspond to the volume obtained from the constant compliance models with $C = C_i^{ave} = 0.0335536$ and $C = C_i^{ave} = 0.0296673$ L/cm H_2O for pre- and post-injury cases, respectively. The dots indicate the real data. The solid vertical lines indicate the time t_{in}.

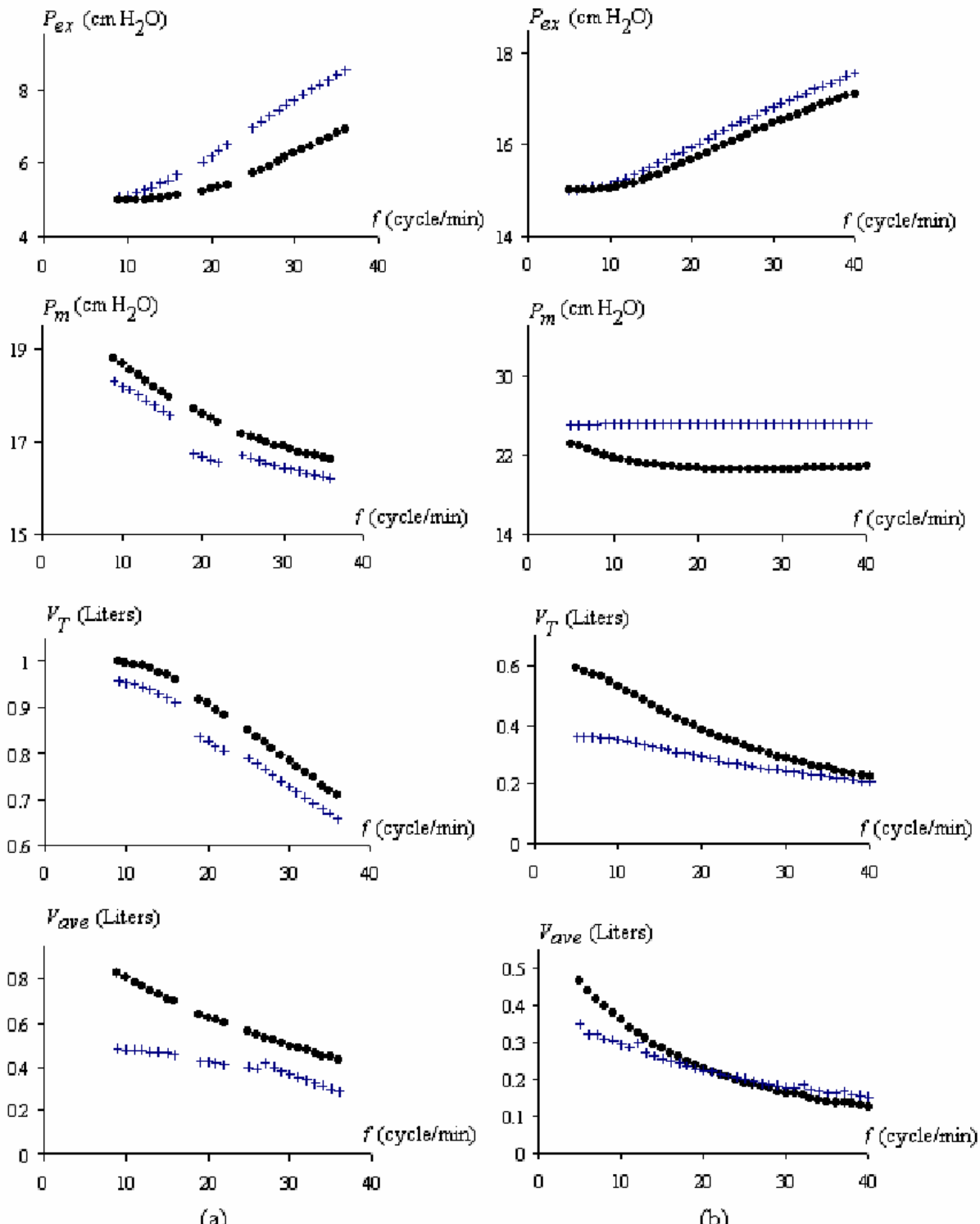

Fig 5. The end-expiratory pressures, tidal volumes, average volumes, and mean alveolar pressures, for both pre-injury (a) and post-injury (b) cases, obtained from the multi-segment model and the constant compliance model, as functions of breathing frequency. The plus signs (+) indicate quantities obtained from the multi-segment model, and the dots (·) indicate those from the constant compliance model.

V_T, average volume V_{ave}, end-expiratory pressure P_x, and mean alveolar pressure P_m, can be calculated. In particular, and are expressed mathematically as

$$V_{ave} = \frac{D}{t_{in}} \sum_{j=1}^{J} \left(\int_{t_{i(j-1)}}^{t_{ij}} V_{i_j}(t)\, dt \right) + \frac{1-D}{t_{tot}-t_{in}} \sum_{k=1}^{K} \left(\int_{t_{e(k-1)}}^{t_{e_k}} V_{e_k}(t)\, dt \right) \quad (15)$$

and

$$P_m = \frac{D}{t_{in}} \sum_{j=1}^{J} \left(\int_{t_{i(j-1)}}^{t_{ij}} \frac{V_{i_j}(t)}{C_{i_j}(V_{i_j}(t)+V_{ex})}\, dt \right) + \frac{1-D}{t_{tot}-t_{in}} \sum_{k=1}^{K} \left(\int_{t_{e(k-1)}}^{t_{e_k}} \frac{V_{e_k}(t)}{C_{e_k}(V_{e_k}(t)+V_{ex})}\, dt \right) + P_{ex} \quad (16)$$

where D denotes the inspiratory time fraction, t_{in}/t_{tot}, or the duty cycle. The intervals, $[t_{i_{(j-1)}}, t_{i_j}]$ and $[t_{e_{(k-1)}}, t_{e_k}]$, are the subintervals of $[0,t_{in}]$ and $[t_{in},t_{tot}]$, respectively, for the different segments in the variable compliance model.

In Table 2, the computed values of the clinical outcomes are given for a particular pig in pre- and post-injury cases using the model equations (9) and (10). In this table, we can see that the tidal volume and average volume decrease with the increasing level of PEEP for both pre- and post-injury cases. At each level of PEEP, the reductions in the tidal and average volumes are approximately 3% in the pre-injury case and approximately 5% in the post-injury case, while the increases in the mean alveolar pressures are more moderate. However, approximately 82% and 70% of the beginning (PEEP = 0) tidal and average volumes still remain at the last level of PEEP (PEEP = 6) in pre- and post-injury cases, respectively.

Comparison of Models

The changes in the clinical outcome variables as functions of the breathing frequency (f) and duty cycle (D) are now investigated. This could yield the optimal choice of and for a clinical setting of P_{set} and P_{peep}. Using the multi-segment variable compliance model and the constant compliance model, numerical simulations for some clinical important outcomes will be carried out as functions of f. Then, the comparisons of these models are made.

We first consider a linear model for pressure controlled ventilation with constant compliance C. This model is given by the differential equations (2) and (3) when $\varepsilon_i = \varepsilon_e = 1$ and $C_i(V_i + V_{ex}) = C_e(V_e + V_{ex}) \equiv C$. Here, we use the average inspiratory compliance C_i^{ave} from the multi-segment model to approximate the value of C. Thus, the average compliance during inspiration was calculated by means of the formula

$$C_i^{ave} = \frac{1}{V_T} \sum_{j=1}^{J} \left(\int_{v_{i(j-1)}+V_{ex}}^{v_{ij}+V_{ex}} C_i(V)\, dV \right), \quad (17)$$

where $v_{i0} = 0$ and $v_{iJ} = V_T$. We can see the effect that the use of a multi-segment variable compliance has on the simulated lung volume in Fig 4. In this figure, the lung volumes are plotted using the multi-segment variable compliance model (solid curve) and the constant compliance model (dashed curve) while the dots indicate real data. We used $C = C_i^{ave} = 0.0335536$ in the pre-injury case, and $C = C_i^{ave} = 0.0296673$ in the post-injury case, in the constant compliance model simulation of a particular pig. The multi-segment model clearly gives a better fit to the real data than the one-segment constant compliance model.

The linkage between the clinical outcome variables and the frequency has been studied by Marini *et al.* using the constant compliance model.[29,30] It was shown that the mathematical model gave robust predictions for the key outcome variables that the clinicians require as the input parameters of mechanical ventilation in order to optimize the desired results. Here, we offer the predictions of the multi-segment model for the key outcome variables as functions of f, and compare these with the predictions of the constant compliance model. In Fig 5, comparisons of the key outcome variables between the two models are shown as functions of frequency. The following values for the physiologic and ventilatory parameters have been chosen: in the pre-injury case; R_i=16 cm H_2O L/s, R_e=17 cm H_2O L/s, P_{set}= 35 cm H_2O, P_{peep}= 5 cm H_2O and D=1/3, and in the post-injury case; R_i=13.75 cm H_2O L/s, R_e=14.25 cm H_2O L/s, P_{set}= 35 cm H_2O, P_{peep}= 15 cm H_2O and D=1/2. The values of the parameters in the compliance functions are listed in Table 1 for both pre- and post-injury cases. The compliance in the constant compliance model simulations is taken to be the average inspiratory compliance of the multi-segment model and ranges from $C_i^{ave} = 0.0335280$ to 0.0337998 L/cmH_2O for f=5 to 40 cycles / min in the pre-injury case and from to 0.0298058 for f=5 to 40 cycles / min in the post-injury case. As can be seen in Fig 5, the plots of the end-expiratory pressure simulated from the two models diverge away from each other as the frequency becomes higher (f>10), while the plots of other outcomes (tidal volume and average volume) resulting from the two models converge toward each other as the frequency increases. A similar comparison can be made of the key outcome variables as functions of duty cycle D.

Limiting Quantities

In this section, we examine the tidal volume V_T, the end expiratory alveolar pressure P_{ex}, the minute

ventilation $V_E = fV_T$, the mean alveolar pressure P_m, and the power (work per minute) $W_m = fW_{br}$, when W_{br} is the work per breath and is given by $P_{set}V_T$. We will investigate these quantities as the breathing frequency f tends to infinity, treating first the one-segment model in which the compliances are linear functions of V.

We define the frequency f cycle/min, and the duty cycle $D = t_{in}/t_{tot}$, so that $t_{in} = 60D/f$ seconds and $t_{ex} = 60(D-1)/f$ seconds. Letting , $\Delta P_i = P_{set} - P_{ex}$ and $\Delta P_e = P_{peep} - P_{ex}$, equations (4) and (5) then become

$$R_i\left(\frac{dV_i}{dt}\right) + \frac{V_i}{a_i + b_i(V_i + V_{ex})} = \Delta P_i,\ 0 \le t \le t_{in} \qquad (18)$$

$$R_e\left(\frac{dV_e}{dt}\right) + \frac{V_e}{a_e + b_e(V_e + V_{ex})} = \Delta P_e,\ t_{in} < t \le t_{tot}. \qquad (19)$$

These can be solved in a straight forward fashion to yield

$$e^{\alpha_i V_i}\left(\frac{A_i + B_i V_i}{A_i}\right)^{-\frac{\beta_i}{B_i}} = e^{\frac{t}{R_i}},\ 0 \le t \le t_{in} \qquad (20)$$

and

$$e^{\alpha_e(V_e - V_T)}\left(\frac{A_e + B_e V_e}{A_e + B_e V_T}\right)^{-\frac{\beta_e}{B_e}} = e^{\frac{t-t_i}{R_e}},\ t_{in} < t \le t_{tot} \qquad (21)$$

where

$$A_i = (a_i + b_i V_{ex})\Delta P_i\ ,\quad A_e = (a_e + b_e V_{ex})\Delta P_e \qquad (22)$$

$$B_i = b_i \Delta P_i - 1\ ,\ B_e = b_e \Delta P_e - 1 \qquad (23)$$

$$\alpha_i = \frac{b_i}{B_i},\ \alpha_e = \frac{b_e}{B_e} \qquad (24)$$

and

$$\beta_i = \frac{a_i + b_i V_{ex}}{B_i},\ \beta_e = \frac{a_e + b_e V_{ex}}{B_e}. \qquad (25)$$

Tidal Volume

We recall that $V_i(t_{in}) = V_T$, so that (20) yields

$$e^{\alpha_i V_T}\left(\frac{A_i + B_i V_T}{A_i}\right)^{-\frac{\beta_i}{B_i}} = e^{\frac{t_{in}}{R_i}}. \qquad (26)$$

We now note that all terms in equation (18) are positive and therefore,

$$P_{ex} \le P_{set} < \infty\ .$$

This means that P_{ex} approaches a finite limit, P_{ex}^{∞}, as $f \to \infty$, and so do the parameters $A\omega$, $B\omega$, $\alpha\omega$ and $\beta\omega$, where $\omega = i$ for inspiration, and e for expiration, which are all dependent on P_{ex}. Using these observations, we may now take the limit as $f \to \infty$ of (26) to obtain

$$\alpha_i^{\infty} V_T^{\infty} = \frac{\beta_i^{\infty}}{B_i^{\infty}} \ln\left(1 + \frac{B_i^{\infty}}{A_i^{\infty}} V_T^{\infty}\right) \qquad (27)$$

where the superscript ∞ denotes the limiting value of each of the above quantities. Notice that the graph of the left hand side of (27) is a straight line through the origin (V_T^{∞} being the independent variable) and the graph of the right hand side is that of a logarithmic function of V_T^{∞}, also passing through the origin. The values of that satisfy (27) are the intersection of the line with the logarithmic curve. Using (22)-(25), we can show that

$$\alpha_i > \frac{\beta_i}{A_i}$$

and therefore the slope at the origin of the straight line is greater than that of the logarithmic curve. Hence, the two curves intersect only at the origin, which means that

$$V_T^{\infty} = \lim_{f \to \infty} V_T = 0. \qquad (28)$$

We note that this is the same result as in the constant compliance case proposed by Marini & Crooke in 1993.[29]

End-expiratory Pressure

We recall that $V_e(t_{tot}) = 0$, so that (21) yields

$$-\alpha_e V_T\left(\frac{A_e}{A_e + B_e V_T}\right)^{-\frac{\beta_e}{B_e}} = e^{\frac{t_e}{R_e}} \qquad (29)$$

From (29), we obtain

$$t_e = R_e\left[\frac{\beta}{B_e}\ln\left(1 + \frac{B_e}{A_e}V_T\right) - \alpha_e V_T\right]. \qquad (30)$$

As f increases, t_e decreases, so that differentiation of both sides of (30) with respect to t_e results in the following equation.

$$1 = R_e\left[\frac{\beta_e}{B_e}\left(\frac{\frac{B_e}{A_e}V_T' + \left(\frac{B_e}{A_e}\right)'V_T}{1 + \frac{B_e}{A_e}V_T}\right) - \alpha_e V_T'\right] + R_e\left[\left(\frac{\beta_e}{B_e}\right)'\ln\left(1 + \frac{B_e}{A_e}V_T\right) - \alpha_e V_T\right]$$

where the prime denotes the derivative with respect to t_e. We now let $f \to \infty$, recalling that $V_T \to 0$, and obtain

$$V_T' \to -\frac{A_e^{\infty}}{(a_e + b_e V_{ex})R_e}\ .$$

Since $t_e = 60(1-D)/f$, one arrives at

$$\frac{dV_T}{df} \to \frac{60(1-D)A_e^{\infty}}{f^2(a_e + b_e V_{ex})R_e} \quad \text{as} \quad f \to \infty \,. \tag{31}$$

On the other hand, the same can be done with the equation (20) to arrive at

$$\frac{dV_T}{df} \to \frac{-60DA_i^{\infty}}{f^2(a_i + b_i V_{ex})R_i} \quad \text{as} \quad f \to \infty \,. \tag{32}$$

Equating (31) and (32), one then obtains

$$\frac{(1-D)A_e^{\infty}}{(a_e + b_e V_{ex})R_e} = \frac{-DA_i^{\infty}}{(a_i + b_i V_{ex})R_i} \,.$$

Using (22), and the corresponding definitions of $\Delta P\omega$, ω=i,e, we then find that

$$P_{ex}^{\infty} = \lim_{f\to\infty} P_{ex} = \frac{DR_e P_{set} + (1-D)R_i P_{peep}}{DR_e + (1-D)R_i} \,. \tag{33}$$

Minute Ventilation

By definition, the minute ventilation is defined as $\dot{V}_E = f\ V_T$. Raising (29) to the power f/α_e, one obtains

$$e^{f\ V_T} = e^{-\frac{60(1-D)}{\alpha_e R_e}} \left(\frac{A_e}{A_e + B_e V_T}\right)^{-\frac{\beta_e f}{\alpha_e B_e}} \,. \tag{34}$$

Letting

$$y = \left(\frac{A_e}{A_e + B_e V_T}\right)^{k f} \,,$$

where $k = -\dfrac{\beta_e}{\alpha_e B_e}$, we see that

$$\ln y = k f \ln\left(\frac{A_e}{A_e + B_e V_T}\right)$$

which tends to an indeterminate form $\infty \cdot 0$ as $f \to \infty$, thus allowing for the use of L'Hopital's rule. This yields

$$\lim_{f\to\infty} \ln y = -\frac{60(1-D)}{b_e R_e} \,. \tag{35}$$

Using (35) while letting $f \to \infty$ in (34) yields

$$\lim_{f\to\infty} f\ V_T = -\frac{60(1-D)}{b_e R_e}\left(B_e^{\infty} + 1\right)$$

or

$$\dot{V}_E^{\infty} = \frac{60D(1-D)(P_{set} - P_{peep})}{DR_e + (1-D)R_i} \tag{36}$$

using (23) and (33).

Mean Alveolar Pressure

The mean alveolar pressure is defined as

$$P_m = \frac{D}{t_{in}} \int_0^{t_{in}} \frac{V_i}{C_i(V_i + V_{ex})}\, dt + \frac{1-D}{t_{ex}} \int_{t_{in}}^{t_{tot}} \frac{V_e}{C_e(V_e + V_{ex})}\, dt + P_{ex} \,. \tag{37}$$

On using equations (18) and (19) to substitute for $\dfrac{V_i}{C_i(V_i + V_{ex})}$ and $\dfrac{V_e}{C_e(V_e + V_{ex})}$, respectively, it is then straight forward to carry out the integrations. As a result, we obtain the following expression for the mean alveolar pressure as a function of f:

$$P_m = D\Delta P_i + (1-D)\Delta P_e + \frac{(R_e - R_i) f\ V_T}{60} + P_{ex} \,.$$

Thus, we let $f \to \infty$ and use (33) and (36) to obtain the limiting value P_m^{∞} of P_m as :

$$P_m^{\infty} = \frac{DR_e P_{set} + (1-D)R_i P_{peep}}{DR_e + (1-D)R_i} \,. \tag{38}$$

We note that $P_m^{\infty} = P_{ex}^{\infty}$ which is the same as that which has been discovered in the constant compliance case.[6]

Power

The power, W_{br}, is defined as the frequency times the work per breath, which has been shown to be equal to $P_{set} V_T$. Therefore

$$\dot{W}_m = f\ P_{set}\ V_T$$

and hence

$$\dot{W}_m^{\infty} = P_{set} \lim_{f\to\infty} f\ V_T = P_{set}\ \dot{V}_E^{\infty} \,.$$

Using (36), one then finds

$$\dot{W}_m^{\infty} = \frac{60D(1-D)(P_{set} - P_{peep})P_{set}}{DR_e + (1-D)R_i} \,. \tag{39}$$

The limits evaluated in this paper are summarized in Table 3. When compared with the limits obtained for the constant compliance models with linear resistive pressure $P_r = RQ$, studied by Marini *et al.* in 1989,[30] and nonlinear resistive pressure $P_r = RQ^{\varepsilon}$ presented by Crooke & Marini in 1993,[6] we notice that there are slight differences. In the previous works, it was assumed that $P_{peep} = 0$ and hence, the formulae given in Table 3 are more general. Also, the calculation of the limiting value P_{ex}^{∞} is new. Otherwise, the limiting values in the case of linear resistive pressure, with constant and variable compliances, are the same.

Furthermore, we note that the limiting values of the key outcome variables obtained from the one-segment model agree with the corresponding values derived for

Table 2. Tidal volumes, end-expiratory pressures, mean alveolar pressures, and average lung volumes for different levels of applied PEEP using the multi-segment model for both pre- and post-injury cases with $P_{set} = 35\ \mathrm{cm\,H_2O}$ and $t_{tot} = 6\,\mathrm{s}$. Here, in the pre-injury case, $R_i = 18\ \mathrm{cm\,H_2O/L/s}$, $R_e = 15\ \mathrm{cm\,H_2O/L/s}$ and D=1/3, and in the post-injury case, $R_i = 13.75\ \mathrm{cm\,H_2O/L/s}$, $R_e = 14.25\ \mathrm{cm\,H_2O/L/s}$ and D=1/2.

PEEP	Pre-injury				Post-injury			
	V_T (Liters)	P_{ex} (cm H_2O)	P_m (cm H_2O)	V_{ave} (Liters)	V_T (Liters)	P_{ex} (cm H_2O)	P_m (cm H_2O)	Vave (Liters)
0.0	1.09810	1.02785	16.7525	0.59194	1.04794	0.128811	15.0985	0.73416
1.0	1.06547	1.91729	17.1220	0.57192	0.98528	1.12434	15.7421	0.69830
2.0	1.03335	2.80452	17.5090	0.55609	0.92513	2.11974	16.3799	0.66341
3.0	1.00180	3.68633	17.9185	0.53436	0.86750	3.11500	17.01200	0.62950
4.0	0.97110	4.60791	18.3972	0.51764	0.81240	4.11019	17.6383	0.59659
5.0	0.94011	5.57522	18.9963	0.50359	0.75982	5.10533	18.2587	0.56468
6.0	0.90943	6.54479	19.5109	0.48709	0.70974	6.10045	18.8735	0.53377

Table 3. Limiting values for variable compliance model.

Outcome Variables	Formulae
Tidal Volume	$V_T^{\infty} = 0$
End-expiratory Pressure	$P_{ex}^{\infty} = \dfrac{DR_e P_{set} + (1-D)R_i P_{peep}}{DR_e + (1-D)R_i}$
Minute Ventilation	$\dot{V}_E^{\infty} = \dfrac{60D(1-D)(P_{set} - P_{peep})}{DR_e + (1-D)R_i}$
Mean Alveolar Pressure	$P_m^{\infty} = P_{ex}^{\infty}$
Power	$\dot{W}_m^{\infty} = \dfrac{60D(1-D)(P_{set} - P_{peep})P_{set}}{DR_e + (1-D)R_i}$

the constant compliance model.[6,30] This is to be expected since it was found that these limiting values are independent of the compliances of the system and only depend on the duty cycle D, the respiratory resistance constants R_i and R_e, and the applied pressures P_{set} and P_{peep}. This leads us to conclude that the same will be found for the multi-segment model. In fact, the outcome variables plotted in Fig 5 do indeed tend to their respective limiting values given by the formulae in Table 3 as $f \to \infty$.

Discussion and Conclusion

It has been recently discovered experimentally and clinically that high pressure mechanical ventilation at volumes above the upper inflection point can cause lung damage. The current ventilatory strategies are aimed at avoiding overdistention and repetitive cycles of recruitment-derecruitment. In such cases, pressure targeted ventilation with high applied PEEP provides a valuable adjunct, since it restricts the maximal alveolar pressure. Hence, these strategies with high applied PEEP may minimize lung injury. Furthermore, pressure limiting ventilatory strategies have been shown to lower mortality in ARDS.

A mathematical model for pressure controlled ventilation with multi-segment variable compliance function has been developed and presented in this paper. The clinical important outcomes can then be computed using this multi-segment model. In Table 2, the tidal volume V_T, end-expiratory pressure P_{ex}, mean alveolar pressure P_m, and average lung volume V_{ave}, are given for different levels of applied PEEP. These calculations illustrate the usefulness of a mathematical model, being a means by which we can experiment with the ventilatory parameters to achieve the desired levels of the clinical outcome variables. Here, we observe that the tidal and average volumes decrease with increasing levels of applied PEEP.

Moreover, the tidal volume diminishes significantly with increasing breathing frequency in the simulation obtained from the constant model. The decline arises from the effects of shortened inspiratory time. The multi-segment model predicts a much smaller dependence of tidal volume on ventilatory frequency. This is potentially important in the clinical setting because it suggests that increasing breathing frequency in the pressure controlled ventilation mode may preserve tidal volume and increase minute ventilation more than that predicted by the constant compliance model.

Although some other researchers on this topic have attempted to fit the P_{el}-V curve with continuous functions, such as the sigmoidal function used by Venegas *et al.*,[14] the resulting models become quite intractable mathematically which is less desirable for analytical proposes. The multi-segment model given in equations (9) and (10) for pressure controlled ventilation has been found to be mathematically tractable and give accurate simulations of mechanical ventilation of normal and injured lungs. The model may be used to study effects of clinical-set inputs on the key ventilatory outcome variables in pigs. The ability to predict these effects can be extremely useful in optimizing ventilatory strategies in the clinical setting for humans.

Acknowledgments

The authors would like to thank the Thailand Research Fund and the National Research Council of Thailand for the financial support.

References

1. Pinhu L, Whitehead T, Evans T and Griffiths M (2003) Ventilator-associated lung injury. *The Lancet* **361**, 332-40.
2. Sharma S, Mullins RJ and Trunkey DD (1996) Ventilatory management of pulmonary contusion patients. *Am J Surg* **171**, 529-32.
3. Wald A, Jason D, Murphy TW and Mazzia VD (1968) A theoretical study of controlled ventilation. *IEEE Trans Biomed Eng* **15**, 237-48.
4. Crooke PS, Kongkul K and Lenbury Y (In Press) Mathematical models for pressure controlled ventilation of Oleic acid-injured pigs. *Math Med Bio*
5. Burke WC, Crooke PS, Marcy TW, Adams AB and Marini JJ (1993) Comparison of mathematical and mechanical models of pressure-controlled ventilation. *J Appl Physiol* **74**, 922-33.
6. Crooke PS and Marini JJ (1993) A nonlinear mathematical model of pressure preset ventilation: description and limiting values for key outcome variables. *Math Mod Meth Appl Sci* **3**, 839-59.
7. Hotchkiss JR, Crooke PS, Adams AB and Marini JJ (1994) Implications of a biphasic two-compartment model of constant flow ventilation for the clinical setting. *J Crit Care* **9**, 114-23.
8. Hotchkiss JR, Crooke PS and Marini JJ (1996) Theoretical interactions between ventilator settings and proximal dead space ventilation during tracheal gas insulflation. *Intensive Care Med* **22**, 1112-9.
9. Morgensterm U and Kaiser S (1995) Mathematical modeling of ventilation mechanics. *Int J Clin Monit Comput* **12**, 105-12.
10. Crooke PS, Head JD and Marini JJ (1996) A general two-compartment model for mechanical ventilation. *Math Comput Model* **24**, 1-18.
11. Silva Neto G, Gerhardt T, Silberg A, Gerhardt T, Claure N, Duara S and Bancalari E (1992) Nonlinear pressure / volume relationship and measurements of lung mechanics in infants. *Pediatr Pulmonol* **12**, 146-152.
12. Nikischin W, Gerhardt T, Everett R and Bancalari E (1998) A new method to analyze lung compliance when pressure-volume relationship is nonlinear. *Am J Respir Crit Care Med*

158, 1052-60.
13. Svantesson C, Sigurdsson S, Larsson A and Jonson B (1998) Effects of recruitment of collapsed lung units on the elastic pressure-volume relationship in anesthetized healthy adults. *Acta Anaesthesiol Scand* **42**, 1149-56.
14. Venegas JG, Harris RS and Simon BA (1998) A comprehensive equation for the pulmonary pressure-volume curve. *J Appl Physiol* **84**, 389-95.
15. Jonson B and Svantesson C (1999) Elastic pressure-volume curves: what information do they convey? *Thorax* **54**, 82-7.
16. Jonson B, Richard J, Straus C, Mancebo J, Lemaire F and Brochard L (1999) Pressure-volume curves and compliance in acute lung injury. *Am J Respir Crit Care Med* **159**, 1172-78.
17. Crooke PS, Marini JJ and Hotchkiss JR (2002) Modeling recruitment manoeuvres with a variable compliance model for pressure controlled ventilation. *J Theor Med* **4**, 197-207.
18. Bowton DL and Kong DL (1989) High tidal volume ventilation produces increased lung water in oleic acid-injured rabbit lungs. *Crit Care Med* **17**, 908-11.
19. Hernandez LA, Coker PJ, May S, Thompson AL and Parker JC (1990) Mechanical ventilation increases microvascular permeability in oleic acid-injured lungs. *J Appl Physiol* **69**, 2057-61.
20. Wilson TA, Anafi RC and Hubmayr RD (2001) Mechanics of edematous lungs. *J Appl Physiol* **90**, 2088-98.
21. Sawada S, Matsuda K, Younger JG, Johnson KJ, Bartlett RH and Hirschl RB (2002) Effects of partial liquid ventilation on unilateral lung injury in dogs. *Chest* **121**, 566-72.
22. Jedlinska B, Mellstrom A, Mansson P, Hartmann M and Jonsson K (2001) Evaluation of splanchnic perfusion and oxygenation during positive end-expiratory pressure ventilation in relation to subcutaneous tissue gases and pH-An experimental study in pigs with oleic acid-induced injury. *Eur Surg Res* **33**, 237-44.
23. Martynowicz MA, Walters BJ and Hubmayr RD (2001) Mechanisms of recruitment in oleic acid-injured lungs. *J Appl Physiol* **90**, 1744-53.
24 Neumann P, Berglund JE, Andersson LG, Maripu E, Magnusson A and Hedenstierna G (2000) Effects of inverse ratio ventilation and positive end-expiratory pressure in oleic acid-induced injury. *Am J Respir Crit Care Med* **161**, 1537-45.
25 Neumann P and Hedenstierna G (2001) Ventilatory support by continuous positive airway pressure breathing improves gas exchange as compared with partial ventilatory support with airway pressure release ventilation. *Anesth Analgesia* **92**, 950-8.
26 Cereda FM, Sparacino ME, Frank AR, Trawoger R and Kolobow T (1999) Efficacy of tracheal gas insufflation in spontaneously breathing sheep with lung injury. *Am J Respir Crit Care Med* **159**, 845-50.
27 Crott S, Mascheroni D, Caironi P, Pelosi P, Ronzoni G, Mondino M, Marini JJ and Gattinoni L (2001) Recruitment and derecruitment during acute respiratory failure-A clinical study. *Am J Respir Crit Care Med* **164**, 131-40.
28 Van der Kloot TE, Blanch L, Youngblood AM, Weinert C, Adams AB, Marini JJ, Shapiro RS and Nahum A (2000) Recruitment maneuvers in three experimental models of acute lung injury-Effect on lung volume and gas exchange. *Am J Respir Crit Care Med* **161**, 1485-94.
29 Marini JJ and Crooke PS (1993) A general mathematical model for respiratory dynamics relevant to the clinical setting. *Am Rev Respir Dis* **147**, 14-24.
30 Marini JJ, Crooke PS and Truwit JD (1989) Determinants and limits of pressure-preset ventilation: a mathematical model of pressure control. *J Appl Physiol* **67**, 1081-92.